



# HHS Public Access

Author manuscript

*Surgery*. Author manuscript; available in PMC 2021 September 07.

Published in final edited form as:

*Surgery*. 2020 January ; 167(1): 189–196. doi:10.1016/j.surg.2019.05.092.

## Overexpression of somatostatin receptor type 2 in neuroendocrine tumors for improved Ga68-DOTATATE imaging and treatment

**Rachael Guenter, BS [Doctoral Graduate Student],**

Department of Surgery, University of Alabama at Birmingham, Birmingham, AL

**Tolulope Aweda, PhD [Scientist I],**

Department of Radiology, University of Alabama at Birmingham School of Medicine, Birmingham, AL

**Danilea M. Carmona Matos, BS, MS,**

HHMI Research Scholar, Department of Surgery, University of Alabama at Birmingham School of Medicine, Birmingham, AL, Medical Student, San Juan Bautista School of Medicine, Caguas, PR

**Samuel Jang, MD [Medical Student and HHMI Research Scholar],**

Department of Surgery, University of Alabama at Birmingham School of Medicine, Birmingham, AL

**Jason Whitt, PhD [Researcher V],**

Department of Surgery, University of Alabama at Birmingham School of Medicine, Birmingham, AL

**Yi-Qiang Cheng [Professor],**

Department of Pharmaceutical Sciences, University of North Texas Health Science Center, Fort Worth, TX

**X. Margaret Liu, PhD [Associate Professor],**

Department of Biomedical Engineering, University of Alabama at Birmingham, Birmingham, AL

**Herbert Chen, MD, FACS [Chairman],**

Department of Surgery, University of Alabama at Birmingham School of Medicine, Birmingham, AL

**Suzanne Lapi, PhD [Professor],**

Department of Radiology, University of Alabama at Birmingham School of Medicine, Birmingham, AL

**Renata Jaskula-Sztul, Ph.D. [Assistant Professor]**

Department of Surgery, University of Alabama at Birmingham School of Medicine, Birmingham, AL

---

Renata Jaskula-Sztul Ph.D. (Corresponding Author) Assistant Professor, Department of Surgery, University of Alabama at Birmingham School of Medicine, Birmingham, AL, 1824 6<sup>th</sup> Avenue South, Wallace Tumor Institute Suite 310H, Birmingham, AL 35233, Phone: 205-975-3507, sztul@uab.edu.

**CONFLICT OF INTEREST:** The authors declare no conflict of interest.

## Abstract

**Background:** Neuroendocrine tumors (NETs) are found throughout the body, including the pancreas (pNETs). These tumors are phenotypically and genetically heterogeneous, and can be difficult to accurately image using current imaging standards. However, PET/CT with radiolabeled somatostatin analogs has shown clinical success, as many NETs overexpress somatostatin receptor subtype 2 (SSTR2). Unfortunately, patients with poorly-differentiated NETs often have a diminished level of SSTR2. We found that histone deacetylase inhibitors (HDAC) inhibitors can upregulate the functional expression of SSTR2.

**Methods:** We evaluated the effect of HDAC inhibitors on SSTR2 expression at the mRNA and protein level in NET cell lines. The effect of HDAC inhibitors on surface-SSTR2 was also investigated by fluorescence-activated cell sorting (FACS) analysis. Changes in SSTR2 expression in NET xenografts after treatment were imaged using Ga68-DOTATATE PET/CT.

**Results:** The functional increase of SSTR2 in NETs after HDAC inhibitor treatment was confirmed through *in vitro* experiments and small animal Ga68-DOTATATE PET/CT imaging. HDAC inhibitors increased SSTR2 transcription and protein expression in NET cell lines. Small animal Ga68-DOTATATE PET/CT imaging confirmed the enhancement of radiopeptide uptake after HDAC inhibitor administration.

**Conclusions:** This study demonstrates a new method to potentially improve imaging and treatments that target SSTR2 in NETs.

## INTRODUCTION:

Neuroendocrine tumors encompass a group of hormone-secreting neoplasms found in various sites throughout the body. Although rare, poorly-differentiated neuroendocrine tumors (NETs) are particularly lethal with ineffective treatment options. Pancreatic neuroendocrine tumors (pNETs) are a subtype of neuroendocrine tumors that originate from endocrine cells of the pancreas and can present as well-differentiated tumors, poorly-differentiated tumors, functional hormone-secreting tumors, or non-functional asymptomatic tumors.<sup>1,2</sup> Globally, the incidence of NETs is steadily increasing with a fivefold increase in the United States over the past thirty years, potentially due to improved cancer screening.<sup>2,3</sup> Unfortunately, there has been no improvement in the 5-year overall survival of patients with unresectable disease.<sup>3,4</sup>

Across all subtypes of neuroendocrine cancer, imaging is a critical component in tumor evaluation, detection, and staging. Computed tomography (CT) and positron emission tomography (PET) using various tracers are available to pNET patients, but with limitations arising from the functional differences between well-differentiated and poorly-differentiated tumors. Two commonly used tracers for neuroendocrine tumor PET imaging include either F-18-fluorodeoxyglucose (F18 FDG) or somatostatin receptor (SST) analogs radiolabeled with Ga-68, such as Ga68-DOTATATE, Ga68-DOTATOC, or Ga68-DOTANOC.<sup>5</sup> F18-FDG has shown higher uptake in poorly-differentiated NETs compared to well-differentiated NETs, but remains insufficient for detection and staging.<sup>5</sup> Grade 1 and grade 2 NETs are often slow growing with low metabolic activity, therefore F18-FDG is not highly concentrated.<sup>5</sup> Aside from F18-FDG, Ga68-DOTATATE is an increasingly used tracer for

NET evaluation based on the high expression of somatostatin receptors in these tumors, with DOTATATE binding with the greatest affinity to somatostatin receptor type 2 (SSTR2). SSTR2 is expressed in 50–100% of pNETs, with higher levels seen in well-differentiated cases versus poorly-differentiated cases.<sup>6</sup> Consequently, the utilization of Ga68-DOTATATE in NETs has proven superior, as exemplified by a study with 25 patients showing that Ga68-DOTATATE had 96% sensitivity for NETs.<sup>5</sup> Although the sensitivity and specificity of SSTR2-specific Ga68-DOTATATE PET/CT imaging has shown to be superior over other imaging modalities, its clinical utility is hampered by variable SSTR2 expression amongst patient. Patients with low SSTR2 expression, are not eligible for SSTR2-based imaging modalities or SSTR2-based peptide receptor radionuclide therapy (PRRT).<sup>7,8</sup> It has been cited that as tumors dedifferentiate, they can no longer concentrate somatostatin analogs, likely due to the fact they lose somatostatin receptor expression.<sup>5,9</sup> Therefore, the ability to reintroduce a high level of functional SSTR2 across all NET patients would allow for improved imaging and assessment of tumor burden, as well as SSTR2-targeting therapies.

Recently, several studies have reported an association between the administration of histone deacetylase (HDAC) inhibitors and increased SSTR2 expression in various cancer cell lines, including pancreatic neuroendocrine cancer cells.<sup>1,10,11</sup> Histone deacetylases (HDACs), play a significant role in the transcriptional regulation of genes and the post-translational modification of proteins.<sup>12</sup> HDAC inhibitors are compounds capable of suppressing the activity of HDACs by binding to their catalytic cores, which leads to chromatin relaxation and thus allowing DNA to be bound by transcription factors.<sup>12,13</sup> Currently in the United States, the Food and Drug Administration (FDA) has approved four HDAC inhibitors in the context of cancer therapy: Vorinostat, Romidepsin, Belinostat, and Panobinostat. Another HDAC inhibitor, valproic acid (VPA), is in cancer clinical trials and FDA approved for neurological applications.<sup>12</sup>

In this study, we tested the hypothesis that HDAC inhibitors can upregulate SSTR2 in pNETs through *in vitro* experiments and small animal PET/CT imaging using Ga68-DOTATATE. The success of this study introduces a potential new method for increasing the presence of SSTR2 in NET patients with low expression to enable both imaging and potential therapies that target SSTR2.

## MATERIALS AND METHODS:

All studies described were reviewed and approved by the Institutional Review Board at the University of Alabama at Birmingham.

### Cell Culture

This study used human pancreatic NET cell lines: BON-1, provided by Dr. Mark Hellmich (The University of Texas Medical Branch at Galveston) and QGP-1 obtained from the Japanese Collection of Research Bioresources Cell Bank (JCRBC). BON-1 cells were derived from a peripancreatic lymph node in a patient with metastatic pancreatic cancer and established by Evers et al.<sup>14–15</sup> BON-1 cells were maintained in glutamine (+) DMEM:F-12 medium (Invitrogen Life Technologies, Carlsbad, CA) supplemented with 10% fetal bovine serum, 100 IU/mL penicillin, and 100 µg/mL streptomycin. QGP-1 cells were derived from

a primary pancreatic tumor and established by Kaku et al.<sup>16</sup> QGP-1 cells were maintained in glutamine (+) RPMI-1640 medium (Invitrogen Life Technologies, Carlsbad, CA) with 10% fetal bovine serum, 100 IU/mL penicillin, and 100 µg/mL streptomycin. The MIA PaCa-2 and PANC1 cell lines, both derived from pancreatic ductal adenocarcinomas, were obtained from ATCC and were maintained as described by Gradiz et al.<sup>17</sup> The human embryonic kidney cell line HEK293, obtained from ATCC, were grown in DMEM medium (Invitrogen Life Technologies, Carlsbad, CA) supplemented with 10% fetal bovine serum, 100 IU/mL penicillin, and 100 µg/mL streptomycin. All cell lines were grown at 37°C and in the presence of humidity and 5% CO<sub>2</sub>.

## Compounds

The HDAC inhibitors FK228 (romidepsin), SAHA (suberoylanilide hydroxamic acid), and VPA (2-propylpentanoic acid) were purchased from Sigma-Aldrich. The Cheng laboratory provided Thailandepsin-A (TDP-A), an analog of FK228, and the Tang laboratory provided AB3.<sup>18,19</sup> All compounds were dissolved in dimethyl sulfoxide (DMSO, Sigma-Aldrich, St. Louis, MO), and stored at -20°C. The varying concentrations of each HDAC inhibitor used throughout this study are based on previously published data.<sup>19</sup>

## Real Time Quantitative PCR

To isolate RNA the RNeasy Plus Mini kit (Qiagen) was used. The concentrations of RNA were determined by NanoDrop 1000 spectrophotometer (Thermo Scientific). Complementary DNA was synthesized from 2µg of total RNA using iScript cDNA Synthesis Kit (Bio-Rad). Real-time quantitative PCR (RT-qPCR) was performed in triplicate on CFX Connect Real-Time PCR Detection System (Bio-Rad). The PCR primer sequences for the SSTR2 forward primer: 5'GAG AAG AAG GTC ACC CGA ATG G 3'; the SSTR2 reverse primer: 5' TTG TCC TGC TTA CTG TCA CTC CGC 3'; the GAPDH forward primer: 5' ACC TGC CAA ATA TGA TGA C 3'; and the GAPDH reverse primer: 5' ACC TGG TGC TCA GTG TAG 3'. Target gene expression was normalized to GAPDH and the Ct method was used to calculate relative gene expression. Error bars show the Standard Error of the Mean (SEM).

## Western Blot Analysis

The basal expression of SSTR2 was assessed in the cell lines: BON-1, QGP-1, MiPaCa, Panc1, and HEK293T. Cells were treated with DMSO as a control or with a HDAC inhibitor. Whole cell lysates were quantified by BCA Protein Assay Kit (Thermo Scientific). The protein samples were denatured and then resolved by a 4–15% Criterion TGX gradient gel (Bio-Rad, Hercules, CA) electrophoresis, transferred onto nitrocellulose membranes (Bio-Rad), blocked in milk (1xPBS, 5% dry skim milk, and 0.05% Tween-20) for 1 hour at room temperature, and incubated in 5% BSA, 1xPBS with anti-SSTR2 primary antibody (Santa Cruz, SSTR2 Antibody (A-8): sc-365502) at a 1:500 dilution overnight at 4°C. Secondary antibody (Cell Signaling, anti-mouse HRP linked antibody 1:1000) was applied for 2 hours at room temperature. The protein bands were detected by Luminata Crescendo Western HRP Substrate (Millipore). GAPDH expression was used as a loading control.

## Flow Cytometry

For the fluorescence-activated cell sorting (FACS) analysis, both BON-1 and HEK293 cell lines were treated with either DMSO as a control or 6nM of the HDAC inhibitor FK228 a total of 48 continuous hours. After treatment, a concentration of  $1 \times 10^6$  cells per replicate were stained for 30 minutes at 37°C with 1µg of an anti-SSTR2 antibody (Novus Biologicals Cat#MAB4224) labeled with Cy5.5 fluorophore (Lumiprobe). Cells were then resuspended in flow buffer (0.5% BSA in sterile PBS) and analyzed using LSRII (LSRII BD Biosciences) to detect the presence of Cy5.5 signal via Alexa Fluor 700 laser. Data was analyzed using FlowJo V5.0 (TreeStar, Inc.).

## Immunohistochemistry

The tissue microarray was prepared by the UAB Research Pathology Core. Biological specimens were obtained from the UAB Surgical Oncology Tumor Bank through an IRB approved protocol. Slides were rehydrated using xylene and ethanol. Antigen retrieval was performed by immersing slides in citrate buffer and placing slides in a pressure cooker for 10 minutes. SSTR2 was detected using an anti-somatostatin receptor 2 antibody [UMB1] - C-terminal (Abcam ab134152) at a 1:200 dilution overnight at 4°C. The next day, an anti-rabbit biotin labeled secondary antibody (Pierce goat anti-rabbit IgG,#31820) was applied to slides for 1 hour at room temperature, followed by 30 minutes of HRP streptavidin incubation. Slides were then stained with DAB Chromogen (Dako Liquid DAB+ substrate K3468) and counter stained with hematoxylin.

## Small Animal Ga68-DOTATATE PET/CT Imaging

Immunocompromised male Nu/Nu mice (Jackson Laboratories, Bar Harbor, ME) were subcutaneously injected with BON-1 cells and xenografts developed to a palpable size in three weeks. Two groups of mice were imaged before (basal images) and after injection of either the vehicle control or the HDAC inhibitor FK228. MicroPET images were acquired by tail vein injection of 120 – 140 µCi (4.4 – 5.2 MBq) of Ga68-DOTATATE, which was injected per mouse before and after intra-tumoral injection of FK228. Static scans were collected at 30 minutes and 90 minutes post-injection. A dose of 12.5mg/kg FK228 was administered to mice receiving the HDAC inhibitor treatment, while non-treated mice received an equal volume of the dissolution vehicle (10% ethanol, 60% PEG, 30% PBS) after the basal microPET images were acquired. Then, mice were imaged again 24 hours after vehicle or FK228 injection. PET and CT images were acquired on a Sofie GNEXT PET/CT scanner. The CT images were reconstructed using a Modified Feldkamp Algorithm. The PET images were reconstructed using a 3D-OSEM (Ordered Subset Expectation Maximization) algorithm (24 subsets and 3 iterations), with random, attenuation, and decay correction. Regions of interest were drawn and the mean and maximum standard uptake values (SUVs) for tumors were determined using the formula:  $SUV = [(MBq/mL) \times (animal\ wt.\ (g))/injected\ dose\ (MBq)]$ .

## Statistical Analysis

All statistical analyses were performed using SPSS (IBM Corp. Released 2017. IBM SPSS Statistics for Windows, Version 25.0. Armonk, NY: IBM Corp.). Differences between

treatments for qPCR were determined through one-way ANOVA followed by a Tukey *post-hoc* test and flow cytometry experiments were analyzed using independent t-tests. Data was normally distributed. *P* values < 0.05 were statistically significant. Error bars show the standard error of the mean (SEM).

## RESULTS

### Variations in Patient SSTR2 Expression limit utility of Ga68-DOTATATE PET/CT

To better understand variations in SSTR2 expression in clinical cases, a tissue microarray (TMA) consisting of tissues from 38 different patients with pNETs was stained for SSTR2 expression. An immunohistochemical analysis revealed that 27 out of 38 (71%) of patients with pNETs had detectable SSTR2 expression. Four representative tissues from patients with pNETs are shown in Figure 1. Both Patient 1 and 2 have grade 2 pNETs with obvious SSTR2 expression as seen by the brown staining in the cytoplasm and on the cell surface. Patient 3 also has a grade 2 pNET, but shows no SSTR2 expression. Patient 4, with a grade 3 pNET, shows minimal cytoplasmic SSTR2 expression. Therefore, this analysis shows that patients with grade 2 or grade 3 pNETs can vary in SSTR2 expression.

### Changes in SSTR2 gene expression after HDAC inhibitor treatment

A continuous 24-hour treatment with each of the HDAC inhibitors FK228, AB3, SAHA, or VPA had a significant effect on SSTR2 mRNA expression, as determined by a one-way ANOVA, in both the QGP-1  $F(10) = 283.998$ ,  $p < 0.001$  and BON-1  $F(8) = 162.586$ ,  $p < 0.001$  pNET cell lines (Figure 2). QGP-1 cells treated with 6nM FK228 (mean  $\pm$  SEM,  $8.89 \pm 0.09$ ,  $p < 0.001$ ), 3 $\mu$ M AB3 (mean  $\pm$  SEM,  $3.89 \pm 0.10$ ,  $p < 0.001$ ), 3 $\mu$ M SAHA (mean  $\pm$  SEM,  $2.50 \pm 0.08$ ,  $p < 0.001$ ), and 4mM VPA (mean  $\pm$  SEM,  $6.05 \pm 0.48$ ,  $p < 0.001$ ) had a significantly higher relative fold expression of SSTR2 mRNA when compared to the DMSO (control) treatment (mean  $\pm$  SEM,  $1.00 \pm 0.01$ ). BON-1 cells treated with 6nM FK228 (mean  $\pm$  SEM,  $6.10 \pm 0.31$ ,  $p < 0.001$ ), 3 $\mu$ M AB3 (mean  $\pm$  SEM,  $4.86 \pm 0.26$ ,  $p < 0.001$ ), 3 $\mu$ M SAHA (mean  $\pm$  SEM,  $5.43 \pm 0.15$ ,  $p < 0.001$ ), and 4mM VPA (mean  $\pm$  SEM,  $3.37 \pm 0.03$ ,  $p < 0.001$ ) had a significantly higher relative fold expression of SSTR2 mRNA when compared to the DMSO (control) treatment (mean  $\pm$  SD,  $1.00 \pm 0.03$ ). GAPDH was used as a housekeeping gene. Tukey *post hoc* tests were performed for treatment comparisons. Graphs show mean  $\pm$  SEM.

### HDAC inhibitor treatment increases SSTR2 protein expression

The basal level of SSTR2 protein expression was compared between two pNET cell lines (QGP-1 and BON-1), two pancreatic adenocarcinoma cell lines (MiaPaCa2 and PANC1), and a non-cancerous cell line (HEK293T) by western blot analysis (Figure 3A). The pNET cell line QGP-1 had higher basal SSTR2 expression than BON-1, thereby QGP-1 could represent a patient with a high level SSTR2 expression and BON-1 could be a patient with medium to low SSTR2 expression. Changes in the amount of SSTR2 protein expression in both QGP-1 and BON-1 cells were assessed using western blotting after a continuous 48-hour treatment with two different doses of the following HDAC inhibitors: TDP-A, FK228, AB3, SAHA, or VPA. There was no evident increase in SSTR2 protein expression after treatment with any of the tested HDAC inhibitors in QGP-1 cells (Figure 3B). However,

there was an evident increase of SSTR2 expression in BON-1 cells after treatment with all HDAC inhibitors (Figure 3C). These results suggest that HDAC inhibitors could likely induce SSTR2 expression in cells that have low or medium SSTR2 expression (BON-1), and may not have a substantial effect on cells with an existing high basal expression of SSTR2 (QGP-1).

### Detection of a higher density of SSTR2 on cell surfaces

To determine if the observed increase in SSTR2 expression after treatment with various HDAC inhibitors applied to the detectable, cell surface expression of SSTR2, fluorescence-activated cell sorting (FACS) using a fluorescently labeled anti-SSTR2 antibody was performed on BON-1 cells. In addition, HEK293 were also analyzed as non-cancerous control cell line (Figure 4). Both cell lines were treated continuously for 48-hours with either 6nM of the HDAC inhibitor FK228 or with DMSO as a control. In BON-1 cells, there was a significant increase in the percent of cells that expressed detectable SSTR2 on the cell surface after treatment with 6nM FK228 (mean  $\pm$  SEM,  $33.7 \pm 0.20$ ,  $t = -52.788$ ,  $p < 0.001$ ), as compared to the DMSO (control) treatment (mean  $\pm$  SEM,  $17.1 \pm 0.24$ ) (Figure 4A). Although the HEK293 cell line showed a significant increase in the percent of cells expressing detectable SSTR2 on the cell surface after treatment with 6nM FK228 (mean  $\pm$  SEM,  $6.35 \pm 0.17$ ,  $t = -22.725$ ,  $p < 0.001$ ) when compared to the DMSO (control) treatment (mean  $\pm$  SEM,  $3.98 \pm 0.07$ ), the overall number of positive cells was 2 to 3 fold lower than the BON-1 cell line (Figure 4B). In summary, these results demonstrate that treatment with HDAC inhibitors could increase the functional density of SSTR2 on the surface of NET cells, indicating the potential for improved binding of Ga68-DOTATATE with PET/CT imaging.

### Ga68-DOTATATE PET/CT Small Animal Imaging of NET Xenografts

Mice bearing BON-1 xenografts demonstrated improved Ga68-DOTATATE binding after HDAC inhibitor administration when imaged using PET/CT (Figure 5). Mice given the vehicle control treatment showed a marginal increase in Ga68-DOTATATE uptake (Figure 5A, C). However, mice treated with the HDAC inhibitor FK228 displayed a significant increase in Ga68-DOTATATE binding (Figure 5B, D). The mice that received HDAC inhibitor administration had an average increase in the standard uptake value (SUV) of  $2.97 \pm 0.68$  at 30 minutes after Ga68-DOTATATE injection, which was determined to be statistically significant. The increase in SUV was  $1.43 \pm 0.06$  (mean  $\pm$  SD) 90 minutes after Ga68-DOTATATE injection, which was not determined to be statistically significant. The group of mice treated with the vehicle control had average SUV increases of only  $0.72 \pm 0.10$  (mean  $\pm$  SD) 30 minutes after Ga68-DOTATATE injection and  $1.33 \pm 0.14$  (mean  $\pm$  SD) 90 minutes after Ga68-DOTATATE injection, indicating improved detection of BON-1 subcutaneous xenografts.

## DISCUSSION:

Neuroendocrine tumors (NETs) are a heterogeneous group of neoplasms that can arise throughout the body from neuroendocrine cells, with 7% cases being classified as pancreatic neuroendocrine tumors (pNETs).<sup>8,20</sup> Imaging pNETs is critical as it provides essential

information for medical management decisions. PET/CT imaging that utilizes the radiotracer Ga68-DOTATATE is highly specific for pNET detection and has therefore improved disease burden assessments and patient management.<sup>8</sup> The success of this technique can be attributed to the specificity of DOTATATE towards somatostatin receptor subtype 2 (SSTR2), a protein overexpressed on most well-differentiated pNET cell membranes. However, patients with pNETs that have little to no SSTR2 expression cannot benefit from this technique. Therefore, in this study we aimed to develop a method of increasing, or re-expressing, SSTR2 in this patient population. In agreement with other studies, we have confirmed that histone deacetylase (HDAC) inhibitors can increase SSTR2 expression in pNET cell lines.<sup>1,10-11</sup> Our results demonstrate that five different HDAC inhibitors (TDP-A, FK228, AB3, SAHA, and VPA) increase SSTR2 expression in pNET cell lines at the transcriptional and translational level. The potential mechanism of induction has been speculated to involve the activation of Notch1 in the Notch pathway.<sup>10,11</sup> The functional modulation of SSTR2 on the surface of pNETs was further confirmed by our octreotide affinity study and *in vivo* PET/CT imaging using Ga68-DOTATATE. The substantial improvement in Ga68-DOTATATE binding by PET/CT after HDAC inhibitor treatment *in vivo* creates evidence that our method could be translatable to the clinic.

It has been previously reported that the expression of SSTR2 correlates with a positive clinical outcome for patients diagnosed with pNETs.<sup>21,22</sup> In addition to enabling the use of Ga68-DOTATATE PET/CT imaging, patients with increased SSTR2 expression could also become eligible for treatment with peptide receptor radionuclide therapy (PRRT). The upregulation, or re-expression, of SSTR2 in pNETs by HDAC inhibitors has the potential to broaden not only imaging, but also the treatment options for patients.

Consistent with previously published data, the TMA analysis included in this study shows that 29% of pNET patients did not have detectable SSTR2. However, only one patient sample on the TMA represented a poorly differentiated pNET because this type of tumor is not commonly resected and therefore tissue is not available to be included on a TMA. The patient tissue from the poorly differentiated pNET did not show SSTR2 expression, which may be attributed the lack of cellular differentiation. Furthermore, our *in vitro* studies only used two available pNET cell lines (QGP-1 and BON-1), in which both had detectable basal SSTR2 expression, as reported in existing literature.<sup>23-25</sup> A pNET cell line representing a patient with undetectable SSTR2 expression is not available to the authors' knowledge. Further studies should be done to expand both *in vitro* and *in vivo* studies to better recapitulate the broad spectrum of SSTR2 expression in patients with pNETs.

The results of this study demonstrate a substantial increase in SSTR2 expression in pNET cell lines after the administration of various HDAC inhibitors. This finding suggests that the epigenetic upregulation of the surface marker SSTR2 could improve precision medicine by potentially enabling the use of Ga68-DOTATATE PET/CT imaging for more patients that have been diagnosed with pNETs, in addition to creating a targetable tumor profile for PRRT.



## ACKNOWLEDGEMENTS:

The authors would like to thank Dr. J. Bart Rose, Wayne Howse, Angela Carter, the UAB Flow Cytometry Core, and the Tissue-Based Translational Research Lab in the Department of Pathology at UAB. Research reported in this publication was supported by the National Center of Advancing Translational Research of the National Institutes of Health under award number UL1TR001417. The content is solely the responsibility of the authors and does not necessarily represent the official views of the National Institutes of Health.

## REFERENCES

1. Wanek J, Gaisberger M, Beyreis M, Mayr C, Helm K, Primavesi F, Jäger T, Di Fazio P, Jakab M, Wagner A, Neureiter D, and Kiesslich T. Pharmacological inhibition of class IIa HDACs by LMK-235 pancreatic neuroendocrine tumor cells. *Int J Mol Sci.* 2018;19:3128.
2. Ro C, Chai W, Yu VE, and Yu R. Pancreatic neuroendocrine tumors: biology, diagnosis, and treatment. *Chin J Cancer.* 2013; 32(6): 312–324. [PubMed: 23237225]
3. Kawasaki K, Fujii M, and Sato T. Gastroenteropancreatic neuroendocrine neoplasms: genes, therapies and models. *Dis Model Mech.* 2018; 11(2): dmm029595.
4. Ilett EE, Langer SW, Olsen IH, Federspiel B, Kjær A, and Knigge U. Neuroendocrine Carcinomas of the Gastroenteropancreatic System: A Comprehensive Review. *Diagnostics* 2015, 5, 119–176. [PubMed: 26854147]
5. Ambrosini V, Campana D, Tomassetti P, Fanti S. <sup>68</sup>Ga-labelled peptides for diagnosis of gastroenteropancreatic NET. *Eur J Nucl Med Mol Imaging.* 2012;39Suppl 1:S52–60. [PubMed: 22388622]
6. Öberg KE, Reubi JC, Kwekkeboom DJ, and Krenning EP. Role of Somatostatins in Gastroenteropancreatic Neuroendocrine Tumor Development and Therapy. *Gastroenterology.* 2010;139:742–753. [PubMed: 20637207]
7. Bodei L, Ambrosini V, Herrmann K, and Modlin I. Current Concepts in <sup>68</sup>Ga-DOTATATE Imaging of Neuroendocrine Neoplasms: Interpretation, Biodistribution, Dosimetry, and Molecular Strategies. *J Nucl Med.* 2017; 58:1718–1726. [PubMed: 28818983]
8. Tirosh A and Kebebew E. The utility of <sup>68</sup>Ga-DOTATATE positron-emission tomography/computed tomography in the diagnosis, management, follow-up and prognosis of neuroendocrine tumors. *Future Oncol.* 2018 1; 14(2): 111–122. [PubMed: 29072093]
9. Hennigs JK, Müller J, Adam M, Spin JM, Riedel E, Graefen M, Bokemeyer C, Sauter G, Huland H, Schlomm T, and Minner S. Loss of Somatostatin Receptor Subtype 2 in Prostate Cancer Is Linked to an Aggressive Cancer Phenotype, High Tumor Cell Proliferation and Predicts Early Metastatic and Biochemical Relapse. *PLoS One.* 2014; 9(7): e100469. [PubMed: 25010045]
10. Sun L, He Q, Tsai C, Lei J, Chen J, Mackey LV, and Coy DH. HDAC inhibitors suppressed small cell lung cancer cell growth and enhanced the suppressive effects of receptor-targeting cytotoxins via upregulating somatostatin receptor II. *Am J Transl Res.* 2018;10(2):545–553. [PubMed: 29511449]
11. Sun L, Qian Q, Sun G, Mackey LV, Fuselier JA, Coy DH, and Yu C. Valproic acid induces NET cell growth arrest and enhances tumor suppression of the receptor-targeted peptide-drug conjugate via activating somatostatin receptor type II. *J Drug Target.* 2016;24(2):169–177. [PubMed: 26211366]
12. Yoon S and Eom GH. HDAC and HDAC inhibitor: from cancer to cardiovascular diseases. *Chonnam Med J.* 2016 1; 52(1): 1–11. [PubMed: 26865995]
13. Eckschlager T, Plch J, Stiborova M, and Hrabeta J. Histone Deacetylase Inhibitors as Anticancer Drugs. *Int J Mol Sci.* 2017; 18(7): 1414.
14. Evers BM, Ishizuka J, Townsend CM Jr., Thompson JCThe human carcinoid cell line, bon. A model system for the study of carcinoid tumors. *Ann. N. Y. Acad. Sci*1994;733:393–406. [PubMed: 7978888]
15. Evers BM, Townsend CM Jr., Upp JR, Allen E, Hurlbut SC, Kim SW, Rajaraman S, Singh P, Reubi JC, Thompson JCEstablishment and characterization of a human carcinoid in nude mice and effect of various agents on tumor growth. *Gastroenterology.* 1991;101:303–311. [PubMed: 1712329]

16. Kaku M, Nishiyama T, Yagawa K, Abe M Establishment of a carcinoembryonic antigen-producing cell line from human pancreatic carcinoma. *Gan.* 1980;71:596–601. [PubMed: 7227711]
17. Gradiz R, Silva HC, Carvalho L, Botelho MF, and Mota-Pinto A. MIA PaCa-2 and PANC-1 – pancreas ductal adenocarcinoma cell lines with neuroendocrine differentiation and somatostatin receptors. *Sci Rep.* 2016; 6: 21648. [PubMed: 26884312]
18. Wang C, Henkes LM, Doughty LB, He M, Wang D, MeyerAlmes FJ, Cheng YQ. Thailandepsins: bacterial products with potent histone deacetylase inhibitory activities and broad-spectrum antiproliferative activities. *J Nat Prod.* 2011; 74: 2031–8. [PubMed: 21793558]
19. Jaskula-Sztul R, Chen G, Dammalapati A, Harrison A, Tang W, Gong S, Chen H. AB3-Loaded and Tumor-Targeted Unimolecular Micelles for Medullary Thyroid Cancer. *Journal of Materials Chemistry B*, 2017, 5, 151–159. [PubMed: 28025618]
20. Lawrence B, Gustafsson BI, Chan A, Svejda B, Kidd M, Modlin IM. The epidemiology of gastroenteropancreatic neuroendocrine tumors. *Endocrinol Metab Clin North Am.* 2011;40:1–18, vii. [PubMed: 21349409]
21. Song KB, Kim SC, Kim JH, Seo DW, Hong SM, Park KM, Hwang DW, Lee JH, Lee YJ. Prognostic value of somatostatin receptor subtypes in pancreatic neuroendocrine tumors. *Pancreas.* 2016;45:187–192. [PubMed: 26474434]
22. Qian ZR, Li T, Ter-Minassian M, Yang J, Chan JA, Brais LK, Masugi Y, Thiaglingam A, Brooks N, Nishihara R., et al. Association between somatostatin receptor expression and clinical outcomes in neuroendocrine tumors. *Pancreas.* 2016;45:1386–1393. [PubMed: 27622342]
23. Brunner P, Jörg AC, Glatz K, Bubendorf L, Radojewski P, Umlauf M, Marincek N, Spanjol PM, Krause T, Dumont RA, Maecke HR, Müller-Brand J, Briel M, Schmitt A, Perren A, Walter MA. The prognostic and predictive value of sstr2-immunohistochemistry and sstr2-targeted imaging in neuroendocrine tumors. *Eur J Nucl Med Mol Imaging.* 2017;44(3):468–475. [PubMed: 27539020]
24. Exner S, Prasad V, Wiedenmann B, Grötzing C. Octreotide Does Not Inhibit Proliferation in Five Neuroendocrine Tumor Cell Lines. *Front Endocrinol (Lausanne).* 2018;9:146. [PubMed: 29681888]
25. Nölting S, Rentsch J, Freitag H, Detjen K, Briest F, Möbs M, Weissmann V, Siegmund B, Auernhammer CJ, Aristizabal Prada ET, Lauseker M, Grossman A, Exner S, Fischer C, Grötzing C, Schrader J, Grabowski P. The selective PI3K $\alpha$  inhibitor BYL719 as a novel therapeutic option for neuroendocrine tumors: Results from multiple cell line models. *PLoS One.* 2017;12(8):e0182852. [PubMed: 28800359]

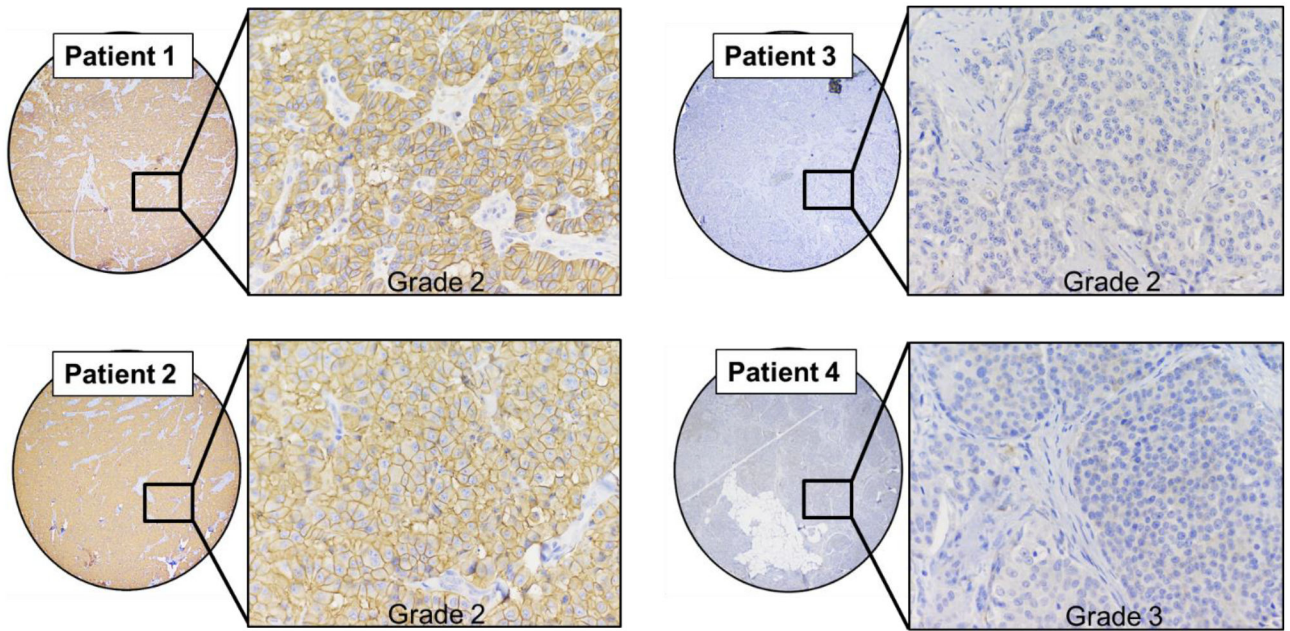


**Figure 1: Tissue microarray of pancreatic neuroendocrine tumors.**

Variations in SSTR2 expression in four representative samples of pNET tissue from patients.

Patient 1 and Patient two show evident SSTR2 staining present in the cytoplasm and cell membrane. Patient 3 and 4 show weak cytoplasmic or nonexistent SSTR2 staining.

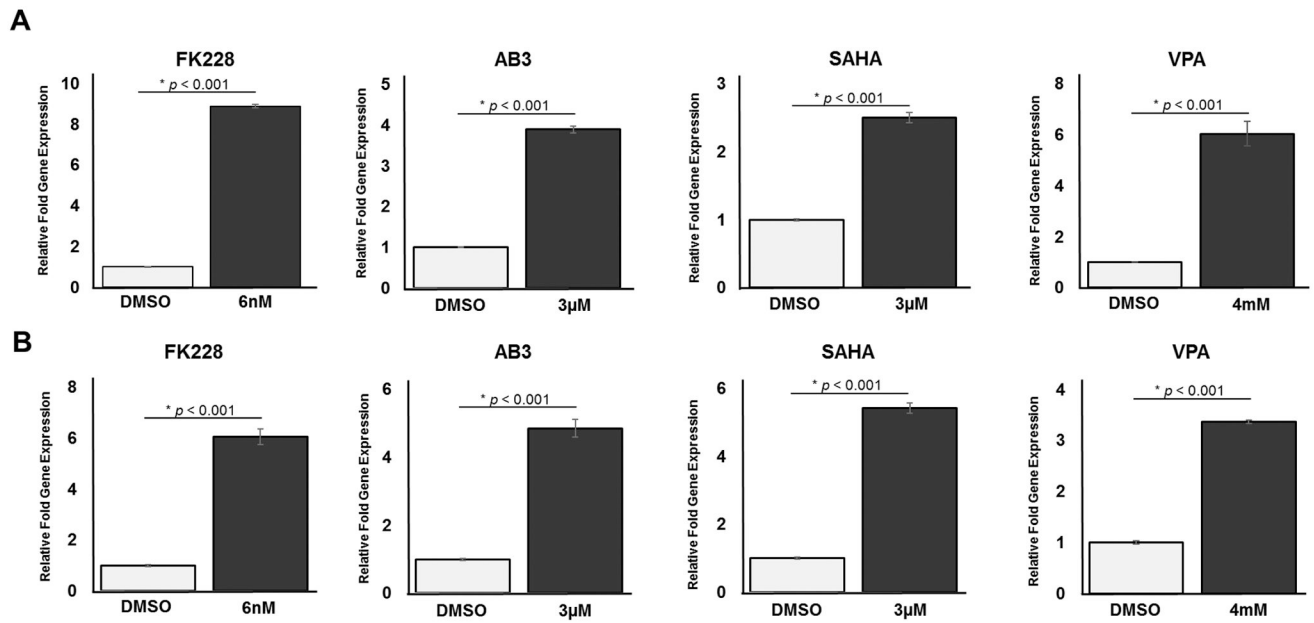


**Figure 2: Upregulation in SSTR2 mRNA Expression.**

(A) QGP-1 cells treated with four different HDAC inhibitors (FK228, AB3, SAHA, or VPA) showed statistically significant increases in SSTR2 mRNA expression as measured by RT-qPCR. (B) BON-1 cells treated with four different HDAC inhibitors (FK228, AB3, SAHA, or VPA) also showed statistically significant increases in SSTR2 mRNA expression.

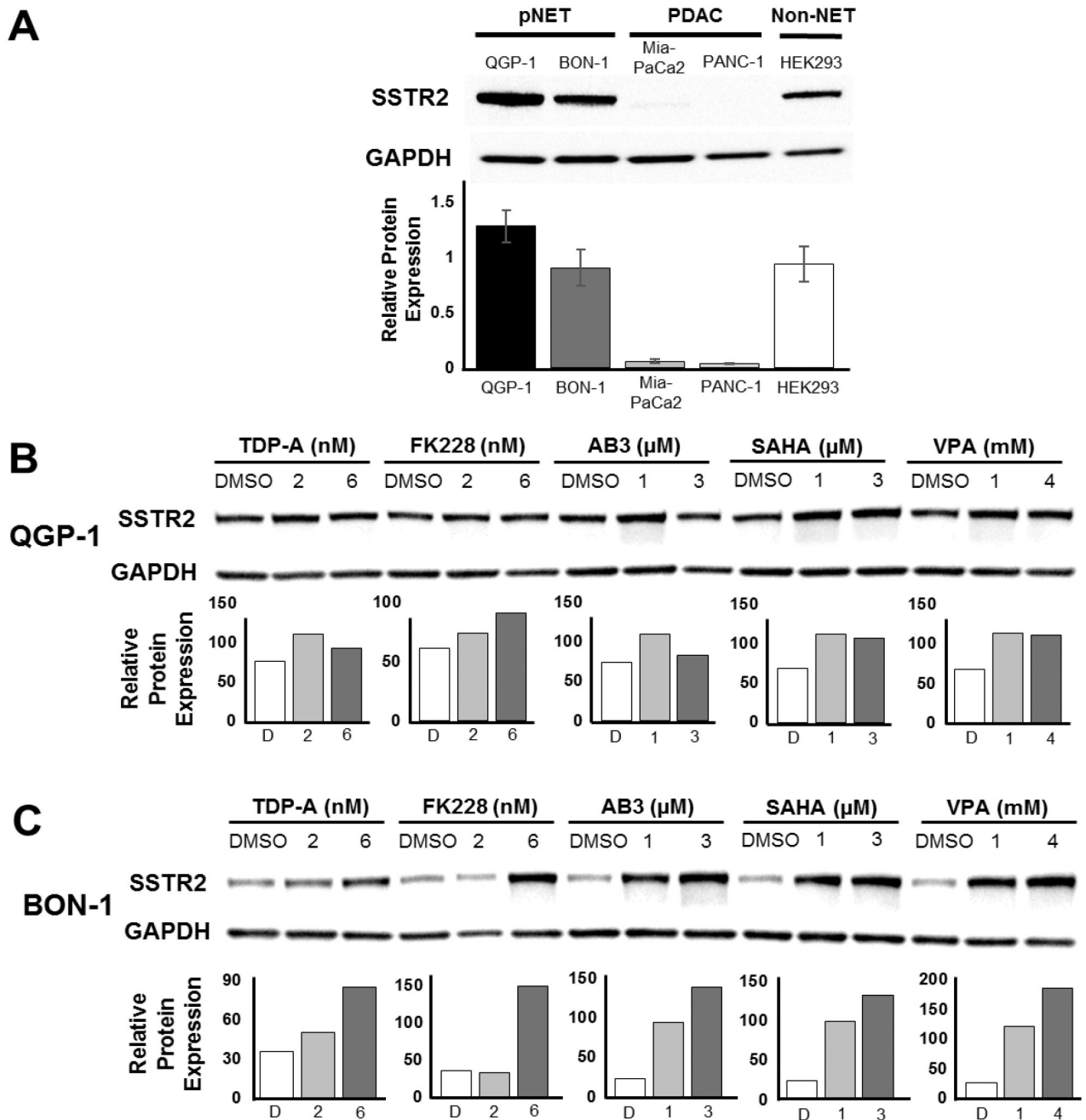


**Figure 3: Changes in SSTR2 protein expression *in vitro*.**

(A) The average basal expression level of SSTR2 in QGP-1 is higher than BON-1. The average basal SSTR2 expression in the pancreatic adenocarcinoma cell lines (MiaPaCa2 and PANC-1) is lower than both pancreatic neuroendocrine tumor cell lines (QGP-1 and BON-1). The non-cancerous cell line HEK293 was run as a positive control. (B) Expression of SSTR2 in QGP-1 (high basal SSTR2 expression) had a 1.7-fold maximum increase of SSTR2 expression with 1mM VPA, whereas (C) BON-1 (low basal SSTR2 expression) had 7.2-fold maximum increase in SSTR2 expression with 4mM VPA.

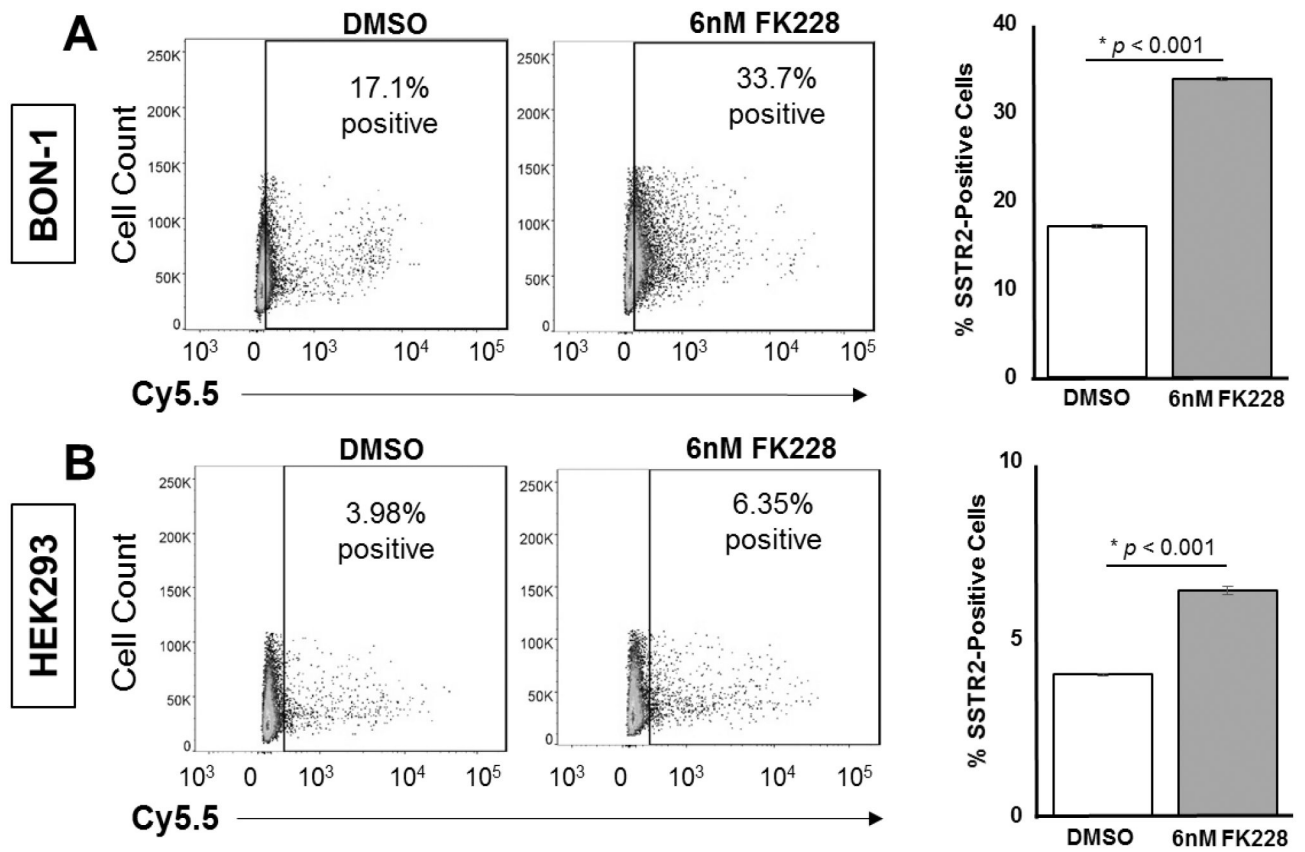


**Figure 4: Increase in surface SSTR2 expression determined by FACS.** Treatment with 6nM FK228 showed a significant increase in surface SSTR2 expression in (A) BON-1 cells and (B) HEK293 cells.

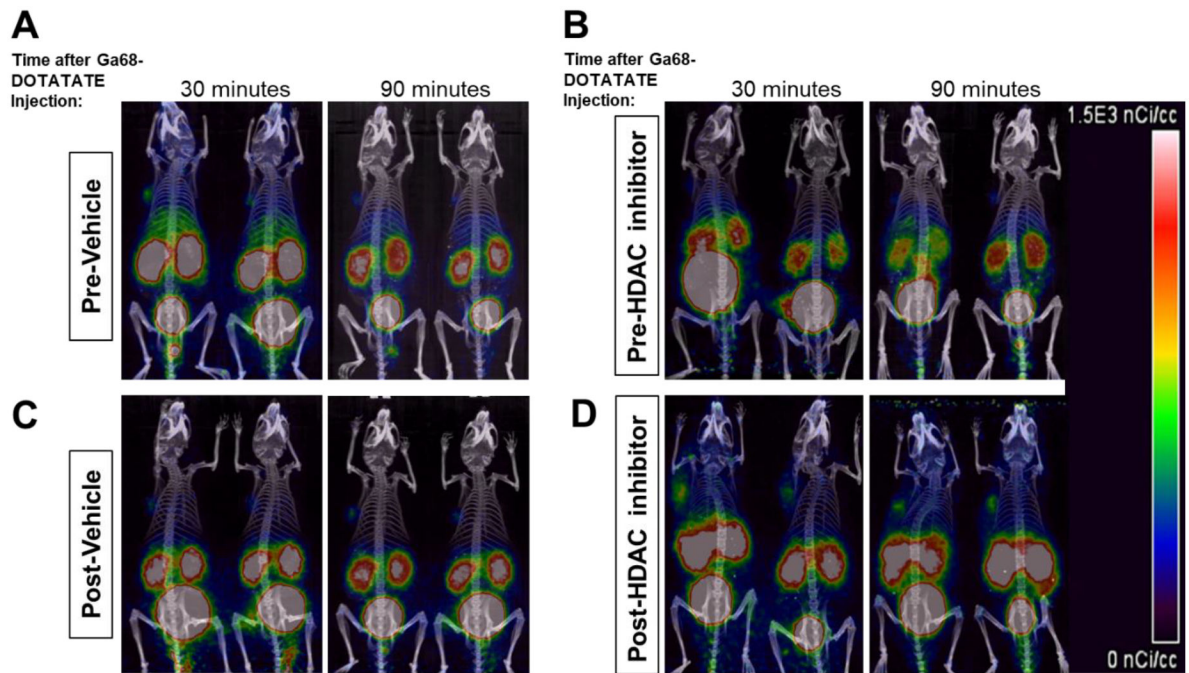


**Figure 5. BON-1 xenografts showed increased Ga68-DOTATATE uptake after HDAC inhibitor (FK228) treatment.**

Ga68-DOTATATE uptake was assessed before and after vehicle and HDAC inhibitor treatment. Prior to treatment, all mice, pre-vehicle (**A**) and pre-HDAC inhibitor (**B**), were imaged 30 minutes and 90 minutes after Ga68-DOTATATE administration. Then, the mice were treated with either the vehicle or treated with the HDAC inhibitor (FK228). After 24 hours, post-vehicle (**C**) and post-HDAC inhibitor (**D**) treated mice were administered Ga68-DOTATATE and imaged at 30 minutes and 90 minutes, respectively. A significant increase in the standard uptake value (SUV) of Ga68-DOTATATE uptake was observed after 30 minutes of Ga68-DOTATATE administration to HDAC inhibitor treated mice. There was also a nonsignificant increase in uptake after 90 minutes of Ga68-DOTATATE.